Numerical analysis of flame behavior in gas turbine combustors using LES

J. Shinjo, Y. Mizobuchi and S. Ogawa
National Aerospace Laboratory of Japan
7-44-1 Jindaiji-higashimachi, Chofu, Tokyo 182-8522 JAPAN

Investigation of lean premixed combustion dynamics in gas turbine combustors is numerically conducted based on Large Eddy Simulation (LES) methodology. The target combustors are a swirl-stabilized combustor and a flame holder model combustor. Unsteady flame behavior is captured inside these combustors. The unstable flame motions are mainly governed by acoustic resonance, velocity field fluctuations and heat release fluctuations. They are all coupled to sustain combustion instabilities. Velocity field analysis around the flame holder in the model combustor is also conducted to understand local flame shapes for further improvement of flame holder designing. It is demonstrated that numerical methods based on LES are effective in comprehending real-scale combustion dynamics in combustors.

1. Introduction

Reduction of NOx emissions is a key issue in modern gas turbine combustor systems due to environmental requirements. Lean premixed combustion is one promising way to reduce emissions because the flame temperature is low compared to conventional non-premixed combustion. However, lean premixed combustion is prone to combustion instabilities, and this sometimes may lead to detrimental damage to combustor systems. In order to attenuate unstable combustion behavior, combustion control is considered effective. Our final goal is to achieve stable combustion over a wide range of operation conditions by passive/active combustion control.

Toward the final goal of combustion control, a detailed understanding of combustion dynamics in combustor systems is necessary because several factors are affecting combustion behavior in a complicated way. Mechanisms of combustion instabilities have been investigated worldwide both experimentally and numerically [1,2]. In combustion experiments, especially for high-pressure tests, measurements are usually difficult to conduct. Visualization is in most cases limited to two-dimensional images and sensors can obtain data at several points. Recent progress in numerical simulation techniques has proven that CFD methods like DNS, RANS and LES can contribute to combustion research in various ways. To understand dynamics in combustor systems, it has been shown that the numerical approach based on LES techniques is effective, although several models are required in the formulation. This allows us to analyze data three-dimensionally.

Here, we numerically simulate practical-scale gas turbine combustor systems to investigate dynamics and mechanisms of unstable combustion in combustor systems. The numerical methods are based on LES techniques and the flamelet model [3,4]. The target combustors are a swirl-stabilized combustor and a flame holder type model combustor installed at National Aerospace Laboratory of Japan (NAL). Details of these combustors are described in the next section.

2. Combustors

In this research we deal with two types of combustor systems.

The first combustor is a swirl-stabilized gas turbine combustor. This type of configuration is generally used in modern gas turbine systems. Figure 1 shows the configuration of the swirl-stabilized combustor analyzed here. The combustion chamber length is L=0.3m and the diameter D=0.15m in this research. The combustor has an inlet section of inner diameter of D_{in}=0.3D and outer diameter D_{out}=0.6D. The exit is contracted to 0.5D. Premixed methane/air at the equivalence ratio of 0.55-0.6 is swirled to the swirl number of about 0.8 in the inlet section. Swirl is numerically given to the flow by adding a hypothetical body force, not by solving swirler vanes. The unburned gas enters the combustion chamber with sudden expansion. The burned gas is accelerated in the contracted exit and goes out of the combustor. The pressure and temperature are set at 1 atm and 400-700K, respectively.

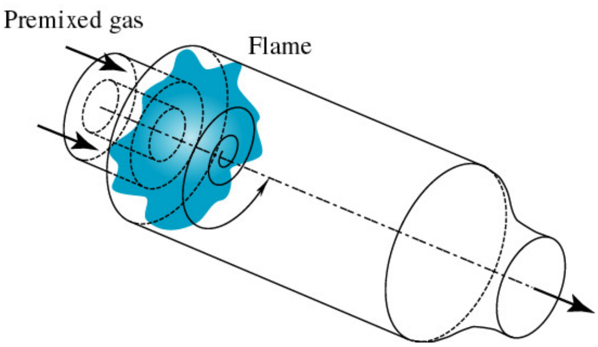

Fig. 1. Swirl-stabilized combustor

We investigate several cases varying flow conditions as shown in Table 1.

Table 1 Calculation conditions for swirl-stabilized combustor

	Case #1	Case #2	Case #3
Inlet temperature (K)	700	400	400
Pressure (atm)	1	1	1
Equivalence ratio	0.55	0.55	0.6
Inlet velocity (m/s)	30	30	30

The second one is the model combustor installed at NAL, which has a cone-shaped flame holder to make the flame region larger. A pilot burner, which injects richer unburned gas to stabilize the flame, is located at the center of the flame holder. The flame holder has eight arms to make recirculation zones behind them. Figure 2 shows the eight flameholder arms and pilot burner installed upstream of the combustion chamber. The combustion chamber has a square cross section, although the inlet section where the flame holder is installed is circular.

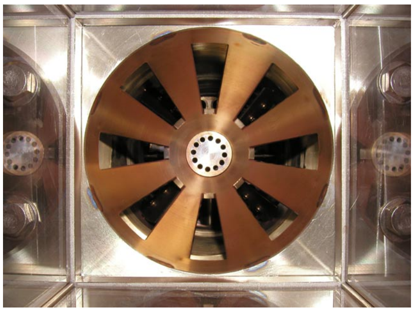

(a)

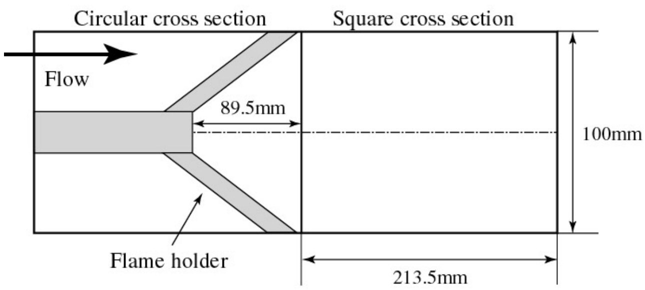

(b)

Fig. 2. Model combustor at NAL
(a) flame holder viewed from combustor exit and (b) dimensions

The combustor is mainly tested by experiment, and this numerical simulation mainly investigates the flame shape and velocity field around the flame holder. In experiment, it is difficult to directly visualize the flame holder region and numerical investigation will contribute to the understanding of the flow around the flame holder region.

In the numerical simulation, injection form the pilot burner is neglected for simplification. The flow conditions are pressure of 1atm, inlet temperature of 700K, inlet velocity of 30m/s and the total equivalence ratio of 0.55.

3. Numerical models

LES techniques are used to capture unsteady turbulent phenomena. In LES, large-scale coherent structures are directly captured by mesh and small-scale (subgrid-scale) eddies are modeled based on the similarity law of turbulence. Spatial filtering operation decomposes the governing equations described below into the two scales.

The governing equations of the system are the three-dimensional Navier-Stokes equations. Compressibility must be included because pressure wave propagation inside the combustor plays an important role in determining flame dynamics.

$$
\begin{aligned}
&\frac{\partial \rho}{\partial t}+\frac{\partial \rho u_j}{\partial x_j}=0\\
&\frac{\partial \rho u_i}{\partial t}+\frac{\partial\left(\rho u_i u_j+\delta_{ij} p\right)}{\partial x_j}=\frac{\partial \tau_{ij}}{\partial x_j}\\
&\frac{\partial E}{\partial t}+\frac{\partial (E+p) u_j}{\partial x_j}=\frac{\partial\left(\tau_{ij} u_i+q_j\right)}{\partial x_j}
\end{aligned}
\tag{1}
$$

In an LES grid system, grid resolution is usually not fine enough to resolve internal structures of flame, thus a flame model should be added to the above equations. The well-known G-equation approach is used in the present formulation. The flame front is assumed to be thin and treated as a discontinuity surface between unburned and burned gases. The propagation speed of the flame surface is called the laminar burning velocity s_L.

$$
\frac{\partial \rho G}{\partial t}+\frac{\partial \rho G u_j}{x_j}=\rho s_L |\nabla G| \tag{2}
$$

LES spatial filtering operation is applied to these governing equations. For example, the filtered momentum equation is

$$
\frac{\partial \bar{\rho}\tilde{u}_i}{\partial t}+\frac{\partial \bar{\rho}\tilde{u}_i\tilde{u}_j}{\partial x_j}=-\frac{\partial \bar{p}\delta_{ij}}{\partial x_j}+\frac{\partial \bar{\tau}_{ij}}{\partial x_j}-\frac{\partial \tau_{ij}^{sgs}}{\partial x_j} \tag{3}
$$

where the bar denotes averaging and the tilde Favre averaging. The last term is an unresolved subgrid term and modeled using the dynamic procedure as

$$
\tau_{ij}^{sgs}=\bar{\rho}\left(\widetilde{u_i u_j}-\tilde{u}_i\tilde{u}_j\right)=-2\bar{\rho}\left(C_s\Delta\right)^2\left|\bar{S}_{ij}\right|\bar{S}_{ij} \tag{4}
$$

where C_s is the dynamic coefficient, Δ the filter scale and $\bar{S}_{ij}$ the resolved strain rate tensor.

The G-equation is also filtered and yields

$$
\frac{\partial \bar{\rho}\tilde{G}}{\partial t}+\frac{\partial \bar{\rho}\tilde{G}\tilde{u}_j}{x_j}=-\frac{\partial}{\partial x_j}\left[\bar{\rho}\left(\widetilde{u_j G}-\tilde{u}_j\tilde{G}\right)\right]+\overline{\rho s_L|\nabla G|} \tag{5}
$$

The flame propagation term of the G-equation is modeled as

$$
\overline{\rho s_L|\nabla G|}=\bar{\rho}\tilde{s}_T\left|\nabla\tilde{G}\right| \tag{6}
$$

where s_T is the turbulent burning velocity. Here, it is given by

$$
\frac{\tilde{s}_T}{s_L}=1+C\left(\frac{u'}{s_L}\right)^n \tag{7}
$$

where u' is the subgrid turbulent intensity. Details of modeling are given for example in [3,4].

Numerical methods are based on the finite-volume discretization. The convective terms are constructed by Roe's upwind numerical flux formulation. The time integration method is two-stage Runge-Kutta integration. Walls are treated as non-slip adiabatic walls. Incoming and outgoing boundary conditions are basically given as non-reflecting conditions. Perfectly non-reflecting conditions, however, do not determine the global mass flow rate. Here, partially non-reflecting conditions are imposed based on Poinsot's method [5] to set the time-averaged mass flow rate at a fixed value. The number of grid point for the swirl-stabilized combustor is about 1 million, and 0.3 million for the NAL model combustor. These grid systems are somewhat coarse to make integration time shorter. Calculations using finer grid systems are underway and will be compared.

4. Results and discussion

4.1. Swirl-stabilized combustor

(a) Flame behavior

In this section, case #1 is mostly analyzed. Figure 3 shows the time-averaged flame shape defined by the G value for case #1. By the swirling motion given to the inlet unburned gas, the flame is stabilized behind the dump plane.

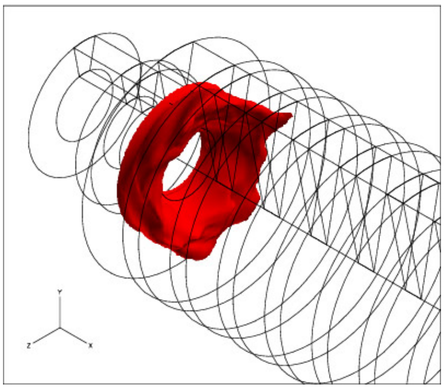

Fig. 3. Averaged flame shape

Figure 4 shows the time-averaged velocity field around the dump plane. A central recirculation zone is formed along the centerline, which pushes the hot burned gas upstream to keep the flame stabilized. Recirculation zones are also created in corner regions due to sudden expansion. This type of flowfield is typically observed in experiments using swirl-stabilized combustors.

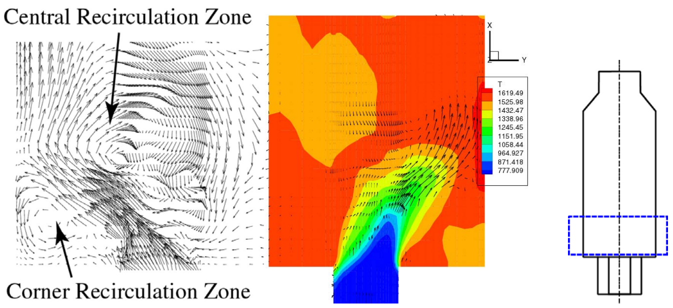

Fig. 4. Averaged velocity field and temperature field around the dump plane

The time-averaged flowfield shown above seems rather simple. But instantaneous flowfield structures are more complicated and change unsteadily. From here, these structures are analyzed.

The temporal pressure trace of case #1 for a certain period is shown in figure 5. The Fast Fourier Transform of the pressure trace is also shown in this figure. The basic frequency is about 740 Hz. The quarter-wave mode frequency, which is usually observed in experiment as a basic mode, can be readily estimated from the combustor length and the speed of sound of burned gas.

$$f_{1/4} = \frac{a}{4L} \approx 700Hz \tag{8}$$

The numerical and analytical frequencies are close and this means the present simulation well produces acoustic resonance in the combustor. Higher modes are also observed as harmonics.

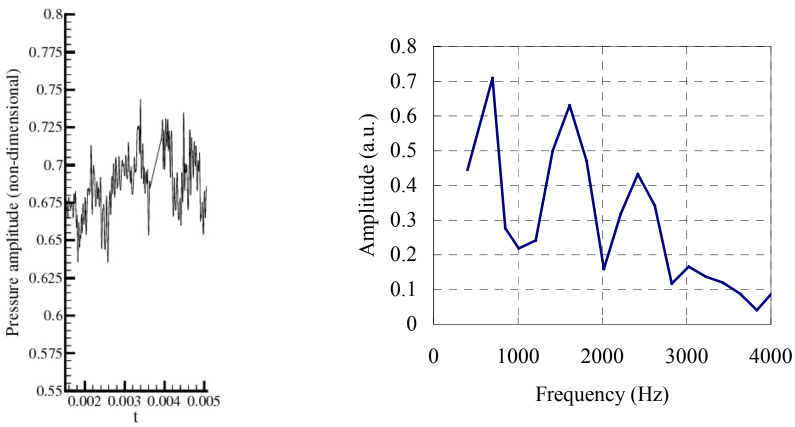

(a) (b)

Fig. 5. (a) Pressure trace and (b) FFT result

Local flame shape is determined by the balance between convective and flame velocities. Inside the combustor, pressure waves are propagating and this causes local velocity field fluctuations. The inlet unburned gas velocity at the dump plane is changing temporally leading to periodic vortex shedding from the dump plane. Figure 6 shows an example sequence of coherent vortical structures and flame shape. Blue structures are vortices identified by the vorticity magnitude. Red surfaces are flame surfaces identified the G value.

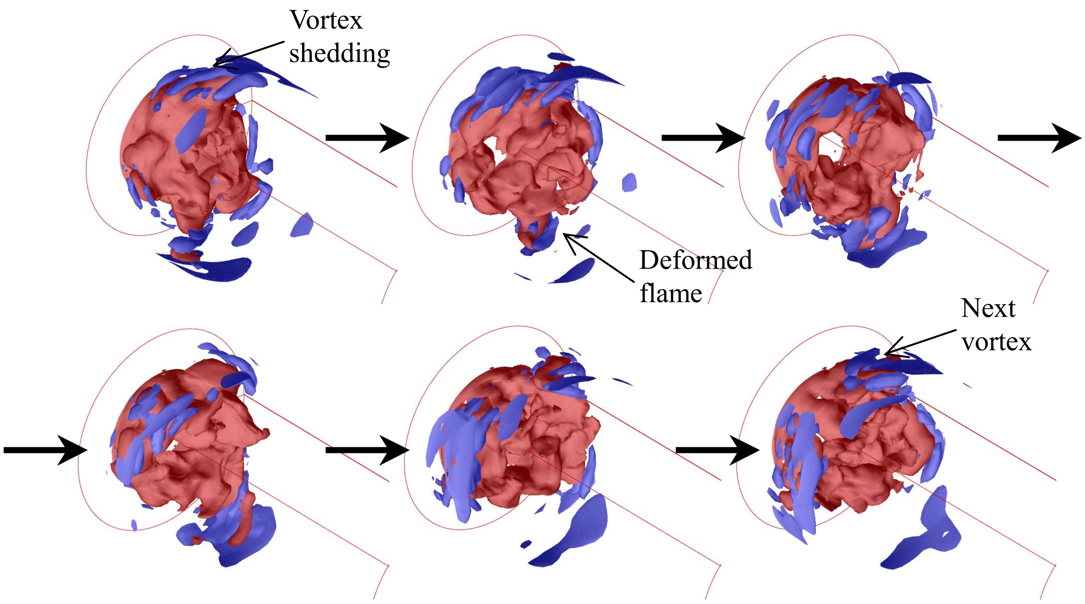

Fig. 6. Vortex/flame interaction: time interval between each shot is about 0.28 ms.

The vortex shedding frequency in this case is determined mostly by acoustic resonance in he combustor. Figure 6 corresponds to nearly one acoustic period of the basic quarter-wave mode. Shear layer instability may also play a role in vortex forming. The relationship between acoustic shedding and shear layer instability is still not clear and should be analyzed in the future.

The flame shape is locally deformed when vortical structures are present in the vicinity. This vortex/flame interaction changes the total flame surface area and flame position. Because heat release occurs at the flame front, fluctuations in flame shape and location are directly connected to heat release fluctuations.

The Rayleigh index is a criterion of combustion system stability. The global Rayleigh index is given by integrating the product of pressure and heat release fluctuations over time and space dimensions. In the present model, local heat release rate is estimated by

$$\dot{q} \propto \rho_u s_T \Delta h A_f / V \tag{9}$$

where ρ_u is unburned density, Δh heat produced by combustion, A_f local flame surface area and V local control volume. The Raleigh index is

$$R = \frac{1}{V}\frac{1}{T}\int_{V,T} p'(\mathbf{x},t)\dot{q}'(\mathbf{x},t)dtdV \tag{10}$$

If the global Rayleigh index is positive, the system is unstable by combustion. For case #1, contours of the local Rayleigh index integrated over time around the dump plane are shown in figure 7.

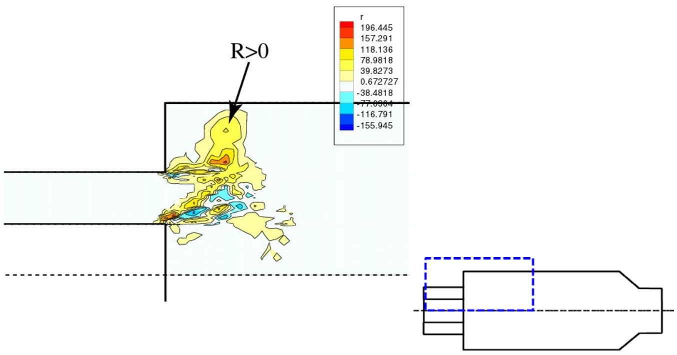

Fig. 7. Local Rayleigh index distribution

In some regions the local Rayleigh index is negative, but in most areas, the index is positive. The global Rayleigh index integrated over space is 2.498(non-dimensional) and positive. Thus heat release and pressure fluctuations are coupled to make the system unstable.

From these results, it can be said that combustion instabilities are driven by interactions between acoustic pressure oscillations, velocity fluctuations leading to vortex shedding and heat release fluctuations. Attenuation of combustion instabilities depends on how to weaken or change these links. This requires a detailed understanding of effects of various parameters, and we need much more calculation cases for this purpose. Below, a preliminary comparison is made between other cases in different conditions.

(b) Effect of inlet temperature and equivalence ratio

Some experimental results indicate that preheating of unburned gas makes combustion more stable [6] to some extent. Comparing pressure traces of case #1 (preheated) and #2 (less preheated), the mean amplitude of case #2 becomes larger. Furthermore, if the global equivalence ratio is increased slightly in case #3, the amplitude becomes again larger. Figure 8 shows the relative pressure amplitude of the three cases. Heat release and thermal expansion ratio may be part of the reason, but further investigation is needed for quantitative evaluation.

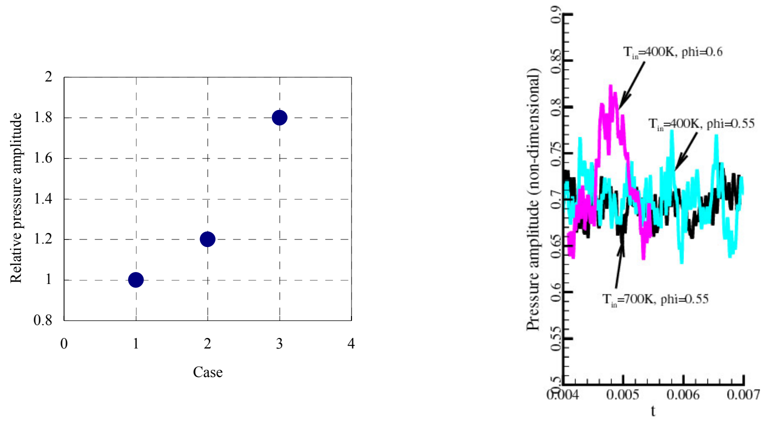

Fig. 8 Parametric variation of pressure amplitude

And also as a future plan, we need to examine the effect of equivalence ratio fluctuations. In real combustor systems, perfectly constant equivalence ratio premixing is almost impossible because fuel and air injection rates can be affected by pressure waves from the combustor. This causes fluctuations in local equivalence ratio, thus local heat release and is expected to make the system unstable. We will soon conduct simulations including this effect.

4.2 NAL model combustor

(a) Flame shape

The model combustor investigated at NAL is simulated using the same methodology.

Figure 9 shows an experimental image of the combustor in operation. The burned gas illuminates brightly, but the flame shape cannot be directly seen. The same LES methodology is applied to this combustor to understand the flame shape around the flame holder.

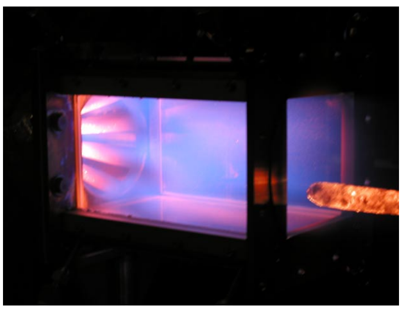

Fig. 9. Experimental image of model combustor in operation. The bar in the right is a gas-sampling probe.

Direct comparison of experimental and numerical flame shapes may be difficult, but some experimental gas-sampling results can help us to understand the averaged flame shape. One example is illustrated here. Shown in figure 10 (a) is the experimental NOx distribution result measured by gas sampling at the combustion chamber entrance. Dashed lines indicate the flame holder arm positions. Because high NOx regions correspond to high temperature regions, combustion seems occurring mainly in areas near the center axis and the arm skirts. Figure 10 (b) shows the numerical result of temperature distribution at the same axial position. The dashed square indicates the measurement area of figure 10 (a). High temperature regions are located at the center and the arm skirt areas. Both results are in good agreement and the present method is able to capture the flame shape.

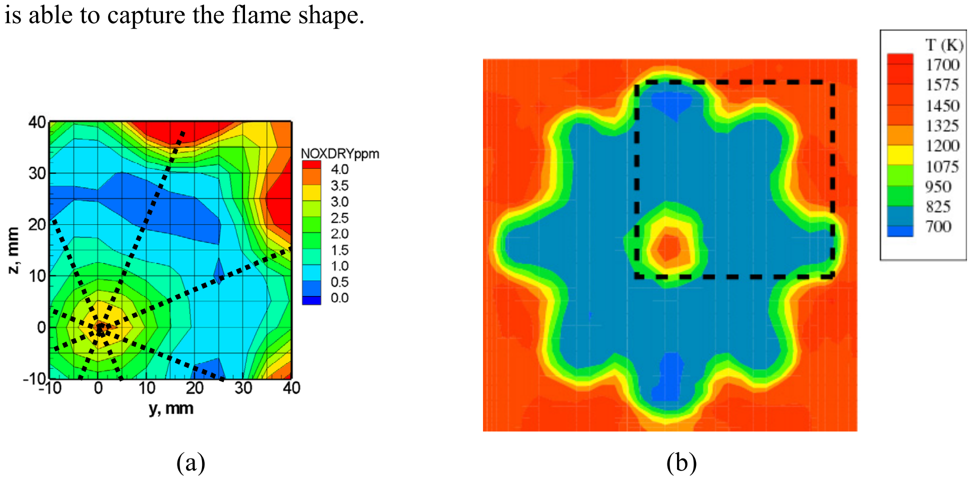

Fig. 10. (a) NOx distribution by experiment and (b) temperature distribution by CFD

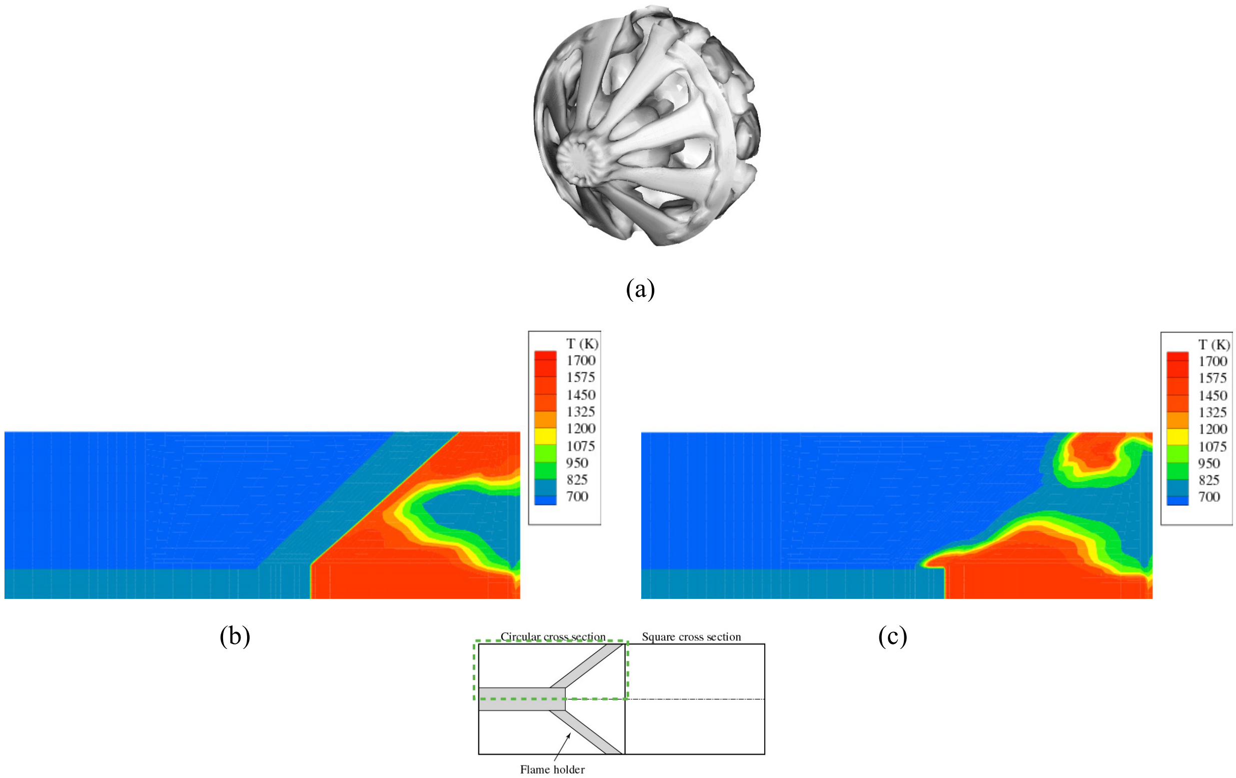

Fig. 11. (a) 3-D Flame shape, (b) temperature distribution behind flame holder arm
and (c) temperature distribution on a plane between arms

Figure 11 shows the three-dimensional flame shape viewed from upstream and the temperature distribution behind the flame holder arm. The unburned gas from the inlet is accelerated when passing through flame holder slits. Behind the flame holder arms, small recirculation and flame regions are created. These recirculation zones are a little smaller than expected. In the pilot burner wake along the center axis, a recirculation zone is also formed.

However, these results may change a little if different wall boundary conditions are imposed because wall heat transfer may have some influence. More experimental data set will be available in the near future and further analysis will be conducted.

5. Conclusions

Numerical investigation of combustion behavior in gas turbine combustors is presented. Two types of combustors are investigated: a swirl-stabilized combustor and a flame holder combustor. LES-based numerical methods employed here are useful in reproducing combustion instabilities in practical-scale combustors.

Unstable combustion behavior is driven by the coupling effects between acoustic resonance, velocity fluctuations and heat fluctuations. If equivalence ratio fluctuations are present, this will also affect the behavior. The coupling between these factors changes depending on flow conditions, and detailed parametric studies are underway.

For the NAL model combustor, the flowfield and flame shape analysis has been conducted and revealed the flowfield structures. Further investigation will be conducted in cooperation with the experimental team.

6. References

[1] Taupin, B., Vauchelles, D., Cabot, G. and Boukhalfa, A., “Experimental study of lean premixed turbulent combustion”, 11th International Symposium on Applications of Laser Techniques to Fluid Mechanics, 2002

[2] Stone, C. and Menon, S., “Swirl control of combustion instabilities in a gas turbine combustor”, Proceedings of the Combustion Institute, 2002

[3] Poinsot, T. and Veynante, D., “Theoretical and numerical combustion”, Edwards, 2001

[4] Peters, N., “Turbulent combustion”, Cambridge University Press, 2000

[5] Poinsot, T. J., and Lele, S. K., “Boundary Conditions for Direct Simulations of Compressible Viscous Flows”, Journal of Computational Physics, 101, pp-104-129, 1992

[6] Lefebvre, A. H., “Gas turbine combustion”, Edwards, 1998